Dalton Transactions

Accepted Manuscript

ROYAL SOCIETY OF CHEMISTRY

www.rsc.org/dalton

Journal Name

RSCPublishing

ARTICLE

Synthesis, Crystal Structures, Electrochemical and Photophysical Properties of Anilido-Benzoxazole Boron Difluoride (ABB) Complexes

Cite this: DOI: 10.1039/xoxxoooooox

Received ooth January 2012,
Accepted ooth January 2012

DOI: 10.1039/xoxxoooooox

www.rsc.org/

Yedukondalu Meesala,[a] Veerababurao Kavala,[a] Hao-Ching Chang,[a] Ting-Shen Kuo,[b] Ching-Fa Yao,*[a] Way-Zen Lee*[a]

A new series of four-ring-fused π-conjugated anilido-benzoxazole boron difluoride (ABB) dyes were synthesized by employing an unsymmetrical bidentate ligand under mild reaction conditions. X-ray structural analysis demonstrated that the four-ring-fused π-conjugated skeleton is nearly coplanar, and almost orthogonal to the side anilido phenyl group with dihedral angles of 74-86°. The synthesized complexes exhibit very bright luminescence in solution (Φ_f = 0.45-0.96 in CH_2Cl_2) and in the solid-state (Φ_f = 0.07-0.37). These complexes show a larger Stokes shift (58-101 nm) than well-known boron dipyrromethene dyes (8-12 nm, in most cases). The role of molecular packing patterns elucidated by the assistance of their X-ray crystal structures rationalizes the solid-state fluorescence. One of the tested compounds displayed aggregation induced emission (AIE). First-principle-based, quantum-chemical studies were carried out on complexes **1**-**6**. Time-dependent DFT (TD-DFT) calculations support the experimental results. The participation of the anilido phenyl moiety and the fluorine atoms was found to be negligible in the LUMO orbitals.

Introduction

Solid-state luminescent dyes have captured tremendous attentions in recent years due to characteristic features that lead to potential uses in organic light-emitting devices (OLEDs),[1] nonlinear optics,[2] fluorescent sensors[3] and biomolecular probes.[4] The most frequently reported luminescent dyes are coumarins,[5] fluoresceins,[6] cyanines,[7] rhodamines,[8] squaraines,[9] and boron dipyrromethene (BODIPY) dyes.[10] BODIPY families are most intriguing because of their outstanding chemical and photophysical properties, such as high molar absorption coefficients, high fluorescence quantum yields and good stability towards light and chemicals.[10] As a result, BODIPY dyes have played an increasingly important role in many fields including fluorescent sensors,[11] photodynamic therapy,[12] laser dyes,[13] and solar cells.[14] However, there is a disadvantage for most BODIPY dyes; that is, they often exhibit relatively small Stokes shifts due to rigid molecular structure with minimal difference between the structures of the ground and excited state.[15] Moreover, their strong luminescent properties in solution tend to be lost in the solid-state because of high planarity, which permits strong intermolecular interactions (e.g., π-π stacking) in solid phase.[16] To minimize π-π stacking in the solid phase, Akkaya et al.,[16a] Qian et al.,[16b] and others[17] have introduced bulky substituent on either meso aryl ring[16a] or BODIPY core.[16b,17] Recently, Chang and Keyes independently demonstrated "Mega-Stokes" BODIPYs.[18] One of the promising strategies to achieve large Stokes shifts and solid-state luminescent properties in BODIPY dyes is to de-symmetrize the bidentate dipyrrin ligand core.[19] Unlike the dipyrrin core present in BODIPY, molecules with unsymmetrical conformation will have large difference between the structures of the ground and excited state.[19] Apart from the dipyrrin framework, several classes of luminescent boron-based dyes have been reported to demonstrate their superior solid-state luminescence properties.[20] Recently, much attention has been paid to four-ring-fused π-conjugated boron chelates because of their flat orientation and rigid π-conjugated molecular structure, which facilitates intense luminescence, good thermal stability and high carrier mobility.[20c-e,21] Very recently, a new class of isoindolin-1-one based BF_2 complexes containing pyridine or benzothiazole groups and hydrazine-Schiff base linked bispyrrole have been prepared by L. Jiao et. al, showed larger Stokes shift.[22] However, their flat π-conjugated molecular orientation may cause serious fluorescence quenching by intermolecular interactions (e.g., π-π stacking) in solid phase. Y. Wang,[23] S. Wang[24] and others[24g] have synthesized solid luminescent boron complexes by introducing phenyl moiety on the central boron atom to overcome this obstacle on four-ring-fused π-conjugated boron chelates. In this contribution, we designed and synthesized the

solid luminescent four-ring-fused π-conjugated anilido-benzoxazole boron (ABB) complexes by encompassing either a phenyl or 2,6-substituted phenyl ring in perpendicular conformation under mild reaction conditions with excellent yields. The X-ray structures, electrochemical and photophysical properties of the ABB dyes are also described.

Results and discussion

Synthesis and Characterization

The four-ring-fused π-conjugated anilido-benzoxazole boron (ABB) complexes **1-6** were synthesized in two steps, starting

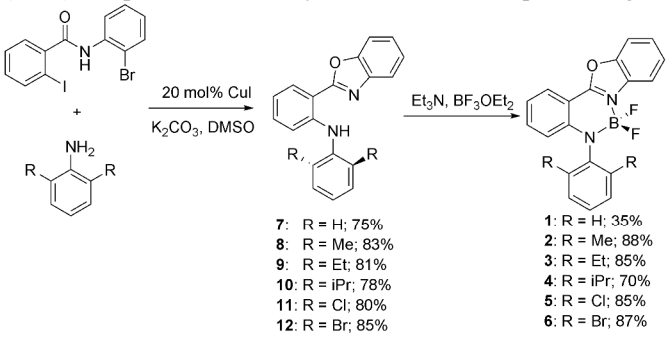

Scheme 1 Synthetic scheme of anilido-benzoxazole complexes **1-6**.

from 2-iodo-*N*-(2-bromophenyl)benzamide as shown in Scheme 1. The required 2-arylbenzoxazole compounds **7-12** were prepared according to a previously reported procedure by treating 2-iodo-*N*-(2-bromophenyl) benzamide with respective aniline and K_2CO_3 in DMSO in the presence of copper iodide as a catalyst at 80°C.[25] Column chromatographic purification on silica afforded **7-12** in 75-85% yield. The compounds **7-12** are soluble in all commonly used solvents and were characterized by various spectroscopic techniques. The data for the known compound **7** is in agreement with the data reported in the literature.[25] The compositions of compounds **7-12** were confirmed by high-resolution mass spectrometry. In the ^{1}H NMR spectrum, the anilido NH signal for **7**, **11** and **12** appears as a broad signal at δ 10.20 ppm and shifts upfield by 0.4 ppm for compounds **8-10** with electron donating substituents at 2

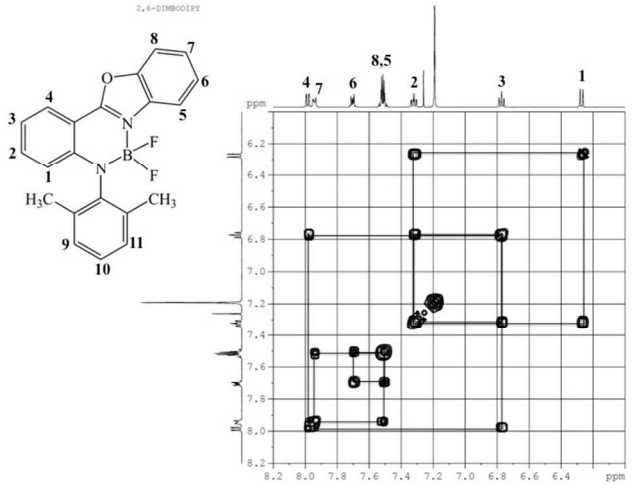

Fig. 1 ^{1}H-^{1}H COSY spectrum of complex **2**.

and 6 positions on the anilido phenyl group. The desired boron difluoride complexes **1-6** were prepared by reacting **7-12** with $BF_3{\cdot}OEt_2$ in the presence of triethyl amine in dry chloroform at room temperature for 2 h. The complexation reaction can be readily monitored by the appearance of a new fluorescent yellow spot on the TLC as well as the disappearance of the downfield proton signal of NH in the ^{1}H NMR spectrum. The crude compounds were subjected to flash chromatography through a silica gel chromatographic column for purification. The pure ABB complexes **1-6** were obtained as yellow solids in 35-87% yield. All these compounds are soluble in conventional organic solvents with good stability. Slow decomposition was observed in the case of **1**. Complexes **1-6** were fully characterized in detail using one- and two-dimensional ^{1}H NMR techniques, ^{13}C, ^{19}F, and ^{11}B NMR, ESI-HRMS, infrared spectroscopies and X-ray crystallography. A representative spectrum of ^{1}H-^{1}H COSY NMR for compound **2** is presented in Fig. 1. The ^{11}B chemical shifts of **1-6** appeared in the range of 1-3 ppm (J = 22.4-27.2 Hz) as well-defined triplets; whereas, the resonances of the ABB dyes displayed at -131 to -133 ppm as broad signals in their ^{19}F NMR spectra. It is noteworthy that the presence of electron-withdrawing groups at 2 and 6 positions on the anilido phenyl group alters the π delocalization. As a result, downfield shifts of the proton signals were observed.

X-ray Structural Analysis

The molecular structures of all boron difluoride complexes **1-6** were determined by X-ray crystallography and are very similar to each other. The ORTEP drawings of **1** and **2-6** are shown in Fig. 2 and Fig. S1, ESI† respectively. Despite their structural similarity, complexes **1-6** crystallized in different space groups. Complexes **1**, **5** and **6** belong to monoclinic $P_{21/n}$ and complex **2** crystallizes in triclinic $P_{\bar{1}}$, whereas complexes **3** and **4** are

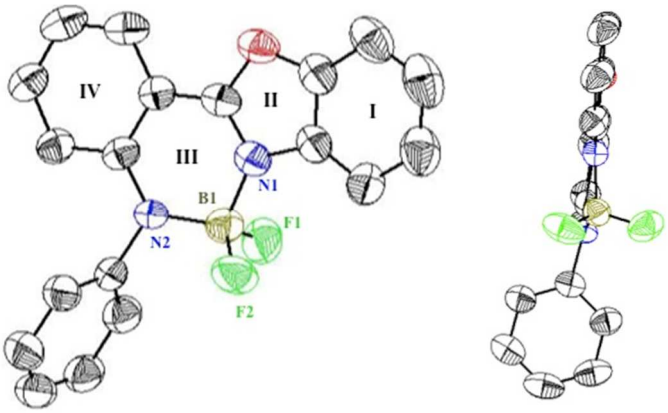

Fig. 2 (Left) ORTEP view of **1** showing the atom labeling scheme. Thermal ellipsoids are plotted at the 50% level. (Right) perpendicular view to highlight the distortion at the B atom. H atoms are omitted for clarity.

in orthorhombic P_{bca}. The diversity of space groups for complexes **1-6** suggests that the packing styles of these complexes are very sensitive to the different substituents on the anilido phenyl group. The X-ray structural analysis of **1-6** revealed that the benzo[*d*]oxazole ring (I,II) and aryl ring (IV) attached to benzo[*d*]oxazole (I,II) moiety and the central six-membered ring (III) containing the boron atom are nearly coplanar, and the anilido phenyl ring is almost orthogonal to the

fused tetracyclic main plane with dihedral angles of 74-86°, the plane defined by the F-B-F atoms is also almost perpendicular to the main plane with the dihedral angle of 87°. The central B atom has slightly distorted tetrahedron geometry on the main plane flanked by two F atoms above and below the plane. In all complexes **1-6**, the B1-N1 distance is longer than the B1-N2 distance matching with the previously reported anilido-pyridine boron difluoride complexes, indicating the structural asymmetry in these molecules.[20] Crystallographic data for **1-6** and selected bond lengths and angles are presented in the Supporting Information (Tables S1 and S2, ESI† respectively). The dihedral angle between the benzo[*d*]oxazole plane and the central six-membered ring (C2-C1-N1-B1) of complex **1** (10°) has a considerable twist than those of complexes **2-6** (0-5°). The fact indicates that introduction of 2,6-substituents on the phenyl ring alters the four-ring-fused π-conjugated framework, and brings the π-system into planarity.

Photophysical Studies

The effects of solvent on the absorption and fluorescence properties of 2-arylbenzoxazole derivatives **7-12** and their boron complexes **1-6** were investigated and the relevant data are listed in Table S3, ESI†. Solvatochromic studies showed only moderate blue shifts in the range of approximately 3-4 nm with an increase in solvent polarity (i.e., hexane → CH_2Cl_2 → acetonitrile) suggesting that the dipole moments of the molecules in the ground and excited states are almost the same.[15] The UV-vis absorption spectra of **1-6** recorded in CH_2Cl_2 are displayed in Fig. 3a and those of 1-5 recorded in the solid-state are shown in Fig. 3b. The maximum absorption wavelength (λ_{max}) of boron complexes **5** and **6**, which contain electron-withdrawing groups at the 2 and 6 positions on the anilido phenyl group, exhibits a slight blue shift relative to those of **2-4** with

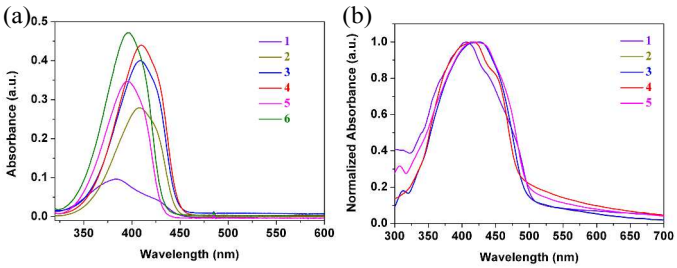

Fig. 3 (a) Absorption spectra of complexes **1-6** recorded in dichloromethane. (b) The normalized absorption spectra of complexes **1-5** in the solid state.

electron-donating groups. Similar observation was found in the absorption spectra of their corresponding free ligands. The λ_{max} of **1-6** shows a red shift with respect to free ligands **7-12**, and the ε values of **1-6** are lower than those of free ligands **7-12** (Table S3, ESI†). The emission properties of free ligands **7-12** and their boron complexes **1-6** were studied in three solvents of varying polarity using both steady state and time-resolved fluorescence techniques. None of the free ligands **7-12** shows visible fluorescence upon irradiation with a UV lamp, whereas all of their boron complexes **1-6** exhibit very bright fluorescence with structured emission bands in solution (Φ_f = 0.45-0.96 in CH_2Cl_2). In addition complexes **1-6** exhibit structureless emission bands in the solid-state (Φ_f = 0.07-0.37). The fluorescence spectra of **1-6** in CH_2Cl_2 and those of **1-5** in the solid-state are shown in Fig. 4a and 4b, respectively, and their photophysical properties recorded in CH_2Cl_2 are summarized in Table 1. The emission maximum (λ_{em}) of **1-6** was hardly affected by the type solvent. Similar to the absorption profiles, the emission band of **5** and **6**, which have electron-withdrawing groups at the 2 and 6 positions on the anilido phenyl group, shows a slight blue shift by 15 nm. The λ_{em} of **2-6** exhibit a red shift in the solid-state when compared with those in hexane by 5-20 nm; whereas, that of **1** shows a blue shift by 17 nm. The opposite shift of the emission band reflects the crystallochromy of **1**. It is noteworthy that all boron complexes except for **1** exhibit a very high fluorescence quantum yield (Φ_f) in three solvents of different polarity. The fluorescence quantum yields of the CH_2Cl_2 solutions of **1-6**, calculated using 9,10-diphenylanthracene as a reference dye (Φ_f = 0.90 ± 0.04 in cyclohexane),[26] were estimated to be 0.45 for **1**, 0.96 for **2**, 0.88 for **3**, 0.93 for **4**, 0.75 for **5**, and 0.59 for **6**. The high Φ_f suggests that the constraint of the orthogonal anilido phenyl moiety caused by ortho substituents increases the rigidity of the boron core, thereby reducing the nonradiative decay (0.01-0.04). All the boron complexes **1-6** exhibited monoexponential decay lifetimes (τ_f) and the lifetimes of **2-6** (4.18-7.80 ns) are much longer than that of **1** (1.37 ns) in

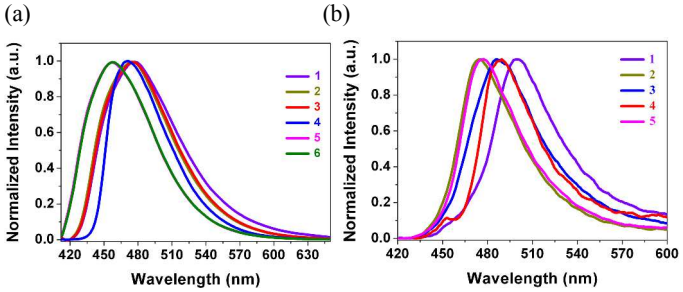

Fig. 4 Normalized emission spectra of complexes (a) **1-6** recorded in dichloromethane. (b) **1-5** recorded in the solid state.

Table 1 Photophysical properties of complexes **1-6**

Dye	CH_2Cl_2[a]							solid-state		
	λ_{abs} (nm) (logε)	λ_{em} (nm)[b]	$\Delta\nu_{st}$ (cm^{-1})	Φ_f[c]	τ_f (ns)[d]	k_r (10^9 s^{-1})[e]	k_{nr} (10^9 s^{-1})[f]	λ_{abs} (nm)	λ_{em} (nm)[g]	Φ_f[h]
1	378 (3.97), 424 (sh)	479	5578	0.45	1.37	0.33	0.40	410	493	0.20
2	408 (4.45)	474	3413	0.96	7.46	0.12	0.01	420	473	0.27
3	408 (4.60)	477	3457	0.88	7.51	0.12	0.01	425	483	0.31
4	410 (4.64)	468	3023	0.93	7.80	0.12	0.008	427	490	0.31
5	396 (4.54)	457	3499	0.75	6.23	0.12	0.04	418	478	0.37
6	397 (4.67)	457	3435	0.59	4.18	0.14	0.12	375, 446 (sh)	464	0.07

[a]Measured at a concentration of 1.0×10^{-5} mol dm^{-3}. [b]The excitation wavelengths (λ_{ex}) were as follows: **1** (380 nm), **2-4** (410 nm) and **5-6** (400 nm). [c]Measured using 9,10-diphenylanthracene as a reference, Φ_f = 0.90 ± 0.04 in cyclohexane. [d]Measured using a single-photon-counting method. [e]Radiative rate constant ($k_r = \Phi_f/\tau_f$). [f]Nonradiative rate constant ($k_{nr} = (1-\Phi_f)/\tau_f$). [g]The λ_{ex} were as follows: **1-5** (400 nm) and **6** (370 nm). [h]Measured using an integrating sphere method.

CH_2Cl_2. The lower Φ_f and shorter τ_f of **1** is due to intramolecular *N*-Ar rotation of the orthogonal anilido phenyl group, which supports nonradiative processes. Recently, Matsui and co-workers observed similar phenomenon for *C*-Ar rotation in their thiazole and pyrimidine based boron complexes.[20a,b,c] In order to understand the aggregation induced emission effect, we investigated the fluorescence properties of **1** and **2** in THF/water mixed solutions of various ratios. When water was gradually added to the THF solution of **1**, the change in the fluorescence color of **1** was observed from yellow-green gradually to blue with decrease in emission intensity. When the water fraction exceeded 85%, the fluorescence color changed from blue to bright yellow-green and λ_{em} (~ 500 nm) was dramatically retrieved with even higher intensity (Fig. S12, ESI†). Notably, both the fluorescence color and the wavelength were unchanged by the addition of water to the THF solution of complex **2**. The radiative (k_r) and nonradiative (k_{nr}) rate constants of **1-6** are in agreement with their quantum yields. The k_{nr} value of **6** (0.12×10^9 s^{-1}) is obviously higher than that of **1-5** due to heavy atom effect of bromine. Unlike most typical BODIPYs, complexes **1-6** showed relatively large Stokes shift (58-126 nm), indicating a change in conformation from the ground state to the excited state due to the deviation from the C_2-symmetric core as found in the dipyrrin chelates.[27] Similar observations were reported in earlier anilido-amine systems.[28] Interestingly, the less sterically hindered **1** exhibited the largest Stokes shift (126 nm) in *n*-hexane because of the exclusion of solvent relaxation.[29]

Solid-state properties

Notably, complexes **1-5** showed bright fluorescence even in the solid-state (Φ_f = 0.20-0.37). The absorption spectra of **1-5** in the solid-state were broader and showed a red shift compared with those in solution, whereas the emission spectra were relatively narrower with a red shift (Fig. 3b and Fig. 4b, respectively). To gain a further understanding of strong fluorescence in the solid-state, the crystal packing of **1-6** was investigated (Fig. S2-S6, ESI†). In the crystal packing of **1** (Fig. 5), two independent stacking columns were formed with intermolecular CH···F and CH/π interactions of 2.62 Å and 2.89 Å, respectively. Also, dimers formed by the paired molecules were observed in each column by π-π interactions for about 3.36 Å (C6···C11). Additional π-π interactions were also observed between dimers about 3.38 Å (C5···C8). However, there are no π-π interactions observed between the stacking columns. Therefore, complex **1** exhibits emission in the solid-state (Φ_f = 0.20). In the case of **2**, two independent stacking columns with dimers with intermolecular CH···F interactions of 2.46 Å and 2.60 Å and CH/π interactions of 2.84 Å were observed (Fig. S2, ESI†). Similar to **1**, the π-π interactions (C7···C9) for the monomers in the dimer in **2** were observed at a distance of 3.36 Å. Nevertheless, the interactions between the dimers of **2** were much weaker than that of **1**. As a result, complex **2** exhibits slightly higher quantum

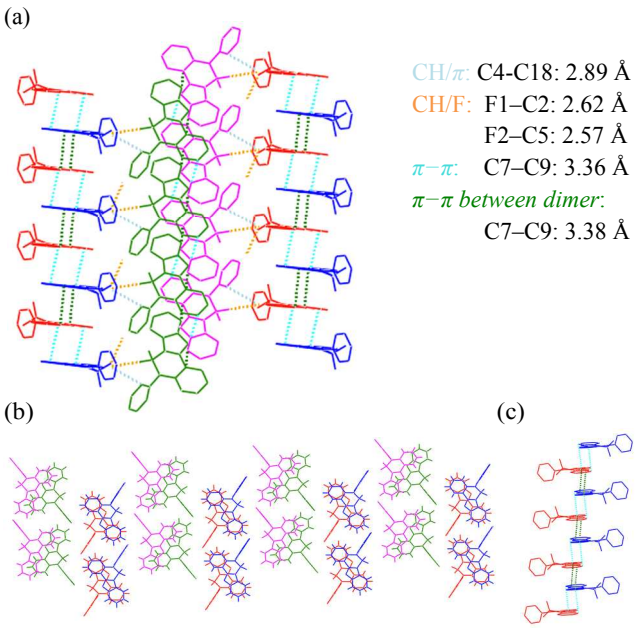

Fig. 5 Crystal packing diagram of **1** (a) top view (b) side view (c) top view of single stacking column arrangement. Hydrogen atoms have been omitted for clarity. The light blue, brown and sky blue dotted lines show intermolecular CH/π interactions, CH/F interactions and $\pi-\pi$ interactions, respectively.

yield (Φ_f = 0.27). For complexes **3** and **4**, two independent columns were still formed. Interestingly, molecules were arranged in a "herring-bone" fashion through CH/F interactions (2.42 Å, 2.58 Å for **3** and 2.59 Å for **4**) and CH/π interactions (2.79 Å for **3** and 2.83 Å, 2.39 Å for **4**). Unlike **1** and **2**, dimers were formed with weak CH···F interactions than strong π-π interactions in the columns. In addition, the highly twisted structures of **3** and **4**, which inhibit π-π interactions, attributed to high quantum yield (Φ_f = 0.31) compared to **1** and **2**. In **5**, dimers were formed and stacked in a "staircase" fashion in each stacking column (Fig. S5, ESI†). However, the intermolecular π-π interactions between dimers only formed through the edge of the dimers in the packing columns resulting in high Φ_f (0.37). The smaller Φ_f of **6** is due to the heavy atom effect of bromine atom.[30] It is clear from the crystal packing of **1-6** that the substituents affect the molecular arrangements in the crystals (Fig. 5, and Fig. S2-S6, ESI†). The high fluorescence properties of boron complexes **1-5** in the solid-state suggest that they might find potential applications in OLED materials.[31]

Electrochemical properties

The electrochemical properties of the anilido-benzoxazole boron difluoride (ABB) dyes **1-6** were investigated by cyclic voltammetry at a scan rate of 0.1 V/s using Bu_4NBF_4 as supporting electrolyte (0.1 M) in CH_2Cl_2. A comparison of the cyclic voltammograms of **1-6** are shown in Fig. 6 and the redox potentials are presented in Table 2. ABB dyes **1-6** exhibited one irreversible reduction wave corresponding to the reduction of the core skeleton. The reduction potentials (E_{red} = -2.15, -2.28, -2.30, -2.33, -2.14, -2.24 V *vs*. Fc/Fc^+ for **1-6**, respectively) are very close to each other, indicating that the substituents at the 2,6-positions of the

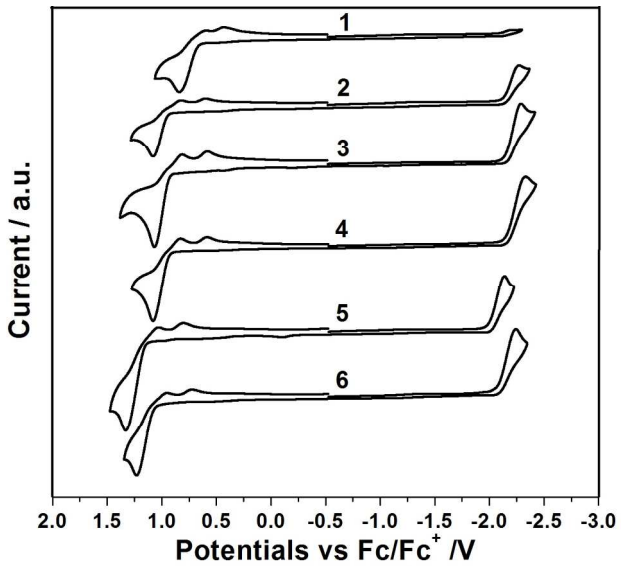

Fig. 6 Cyclic voltammograms of complexes **1-6** in dichloromethane containing 0.1 M Bu_4NBF_4 as supporting electrolyte recorded at 0.1 V s^{-1} scan speed.

perpendicularly oriented anilido phenyl group do not greatly affect the electron density of the conjugated π-system. However, complexes **2-4** with electron donating substituents display slightly negative shift on their reduction waves in comparison with complex **1**, suggesting the involvement of the anilido phenyl group in the redox process. Compared with complex **6** which has bromo substituents, complex **5** with chloro substituents exhibits more positive reduction display slightly negative shift on their reduction waves in comparison with complex **1**, suggesting the involvement of the anilido phenyl group in the redox process. Compared with complex **6**, which has bromo substituents, complex **5** with chloro substituents exhibit more positive reduction potential. From the reduction potentials, the lowest unoccupied molecular orbital (LUMO) energy levels were calculated to be in the range of -2.47 to -2.66 eV.[31] Complexes **1-6** showed one irreversible reduction wave with

Table 2 Electrochemical data of complexes **1-6** recorded in dichloromethane.

Dye	$E_{ox}^{1/2}$ vs. Fc/Fc^+(V)	E_{red} vs. Fc/Fc^+(V)	HOMO (eV)	LUMO (eV)
1	+0.43/+0.71	-2.15	-5.51	-2.65
2	+0.59/+0.95	-2.28	-5.75	-2.52
3	+0.57/+0.94	-2.30	-5.74	-2.50
4	+0.56/+0.96	-2.33	-5.76	-2.47
5	+0.80/+1.18	-2.14	-5.98	-2.66
6	+0.72/+1.14	-2.24	-5.94	-2.56

reduction potential $E_{ox}^{1/2}$ at +0.71, +0.95, +0.94, +0.96, +1.18, +1.14 V *vs*. Fc/Fc^+, respectively. The reduction potential of **1-6** is corresponding to the oxidation of the π-conjugated core along with one ill-defined oxidation peak. On the basis of the oxidation potentials, the energy level of the highest occupied molecular orbital (HOMO) of **1-6** was calculated to be in the range between -5.51 eV to -5.98 eV.[31] The energy levels (HOMO and LUMO) of **1-6** are in general agreement both in terms of trend and magnitude with those obtained by DFT calculations.

Theoretical Calculations

To understand the absorption properties of the ABB dyes **1-6**, we carried out DFT quantum-chemical calculations. The equilibrium structures were optimized at DFT/B3LYP level using a 6-31 G(d,p) basis set. TD-DFT calculations in CH_2Cl_2 (using the CPCM polarizable conductor calculation model) were performed using a B3LYP/6-311+G(2d,p) method. The calculated λ_{max}, main orbital transition, and oscillator strength f are presented in Table S4, ESI†. For all complexes, the absorptions are mostly attributed to HOMO-LUMO transitions. According to the TD-DFT calculations, the calculated UV-vis spectra of the boron complexes **1-6** are closely matched with the experimental results. The calculated λ_{max} increases in the order of 397 (410) for **4** > 396 (408) for **3** ≥ 395 (408 nm) for **2** > 387 (397) for **6** > 387 (396) nm for **5**, and the calculated λ_{max} values are in good agreement with the experimental values (in brackets). As shown in Fig. 7, LUMO orbitals of all complexes are

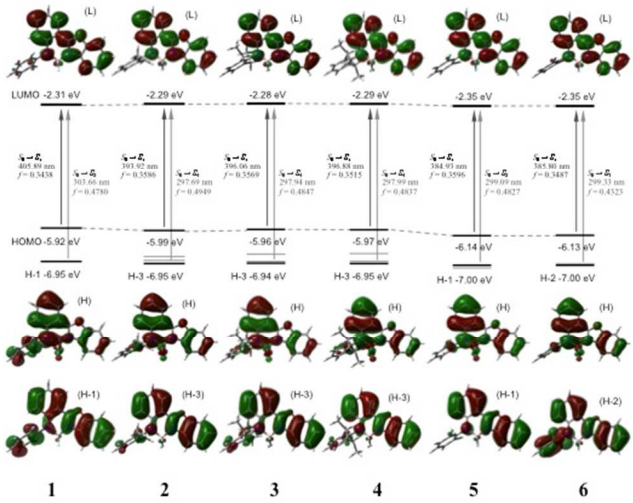

Fig. 7 Calculated molecular orbitals and energy levels of complexes **1-6**.

close to each other, being in the range of -2.28 eV to -2.35 eV. The electron density mainly delocalizes on the four-ring-fused π-conjugated skeleton, contribution from perpendicular oriented anilido phenyl group and fluorine atoms is less than 1% in their LUMO frontier orbitals suggesting that the substituents at 2,6-positions of the anilido phenyl group do not contribute to the LUMOs and can only slightly tune the energy levels. This result is consistent with observations made in the cyclic voltammetry. In the HOMOs, contribution from the perpendicular oriented anilido phenyl group and the fluorine atoms significantly increased than their LUMOs. The HOMO levels of complexes **2-4**, which possess electron-

donating groups at 2,6-positions of the phenyl anilido group, are significantly increased in comparison with those of complexes **5** and **6** with electron-withdrawing substituents. The HOMO-LUMO energy gaps follow the same trend as that obtained from cyclic voltammetry redox potential values. The substantial increase of the energy gap between HOMO and LUMO of complexes **5** and **6** results in blue shift in UV-vis spectra. The minimal changes in the HOMOs and LUMOs of complexes **2**-**6**, which was reflected in their emission profile by retaining their spectra identical when increasing the solvent polarity from hexane to dichloromethane and finally to acetonitrile (Table S3, ESI†), suggest that no intramolecular charge transfer takes place.

Conclusions

In summary, we have synthesized a series of four-ring-fused π-conjugated anilido-benzoxazole boron difluoride (ABB) dyes in two steps starting from 2-iodo-*N*-(2-bromophenyl)benzamide under simple reaction conditions. X-ray structural analysis indicates that four rings fused together with boron-bridge in a π-conjugation framework are in a nearly coplanar orientation and anilido phenly group connected to this frame work is almost orthogonal with the dihedral angle of 74-86°. By introducing orthogonal anilido phenyl group on the rigid core skeleton enables them to be very bright and strongly fluorescent in solution and the solid-state. The substituents at the 2 and 6 positions of the orthogonal anilido phenyl group alter the electronic properties, which are reflected in various spectroscopic, electrochemical and optical properties. All these complexes are exhibiting relatively large Stokes shifts (58-101 nm) as compared to the popular boron-dipyrromethene complexes (8-12 nm). The solid-state fluorescence of **1**-**6** was interpreted from their molecular packing patterns revealed by the assistance of their crystal structures. The electrochemical studies as well as quantum-mechanical studies at the DFT level indicated that the contribution of orbital delocalization mainly from four-ring-fused π-conjugated skeleton unit.

Experimental Section

All of commercially available reagents and solvents are analytically pure used in the experiment without any further purification unless otherwise specified. The solvents used for photophysical measurements were of HPLC grade. Column chromatography was performed on silica gel (60-120 mesh). 2-(Benzo[*d*]oxazol-2-yl)-*N*-phenylaniline was synthesized according to literature method. ^{1}H, ^{13}C, ^{11}B and ^{19}F NMR spectra were run on a Bruker Avance-400 MHz FT NMR spectrometer with tetramethylsilane (^{1}H) as an internal standard. IR spectra were recorded using solution cell on a Perkin-Elmer Paragon 500 spectrometer. ESI-MS spectra were recorded on a Thermo Finnigan LCQ Advantage spectrometer. UV-vis absorption spectra were recorded using an Agilent 8453 spectrophotometer. Emission and excitation spectra were obtained on a Jobin-Yvon FL3-21 Horiba Fluorolog fluorescence spectrophotometer. Fluorescence decay surfaces were determined by single photon counting technique using a CD-900 Edinburgh spectrometer. The fluorescence quantum yields in solution were measured relative to 9,10-diphenylanthracence (DPA) in cyclohexane as a standard reference (λ_{ex} = 325 nm, Φ_f = 0.90 ± 0.04) at room temperature. Solid-state emission quantum yields were determined with the use of Jobin-Yvon FL3-21 Horiba Fluorolog fluorimeter equipped with an integrated sphere. Cyclic voltammetric (CV) studies were carried out with Epsilon e2 electrochemical analyzer system utilizing the three electrode configuration consisting of a glassy carbon (working electrode), platinum wire (auxiliary electrode) and silver (reference electrode) electrodes in dry dichloromethane using 0.1 M tetra butylammonium tetrafluoroborate as supporting electrolyte. The reported potentials are referenced with respect to the ferrocenium/ferrocene couple, which was recorded at the end of each experiment. The solution was deaerated by bubbling argon gas, and during the acquisition argon was slowly flowed above the solution.

X-ray Diffraction: Single crystals of **1**-**6** suitable for X-ray diffraction analysis were grown by hexane vapors into a dichloromethane solution. The diffraction data were collected on a Bruker-Nonius Kappa CCD diffractometer employing graphite-monochromated Mo *K*α radiation at 200 K and the θ-2θ scan mode. The structures were solved by direct methods and refined by full-matrix least-squares methods on all F2 data (SHELX-97). Non-hydrogen atoms were refined anisotropically. The positions of hydrogen atoms were calculated and refined isotropically. The CCDC deposition numbers for complexes **1**-**6** are 966878 - 966883.

General Procedure for 2-arylbenzoxazole (7-12):

Copper iodide (20 mol%) and potassium carbonate (2 mmol) were added to a solution of 2-iodo-*N*-(2-bromoaryl)-benzamide (1 mmol) and a amine (1.5 mmol) in DMSO. The reaction mixture was then heated at 80°C until the reaction was complete. The reaction mixture was then extracted with ethyl acetate and the ethyl acetate solution was washed with a brine solution. The organic layer was separated, dried over anhydrous $MgSO_4$ and concentrated under vacuum to obtain the crude product. The crude product was further purified by silica gel column chromatography with hexane/ethyl acetate (95:5), which afforded pure 2-aryl benzoxazoles **7**-**12** in 75-85% yield.

General Procedure for anilido-benzoxazole boron difluoride (ABB) dyes (1-6):

2-aryl benzoxazoles **7**-**12** (1 mmol) were dissolved in dry chloroform (50 mL). Triethylamine (10 mmol) and boron trifluoride diethyl ether complex (15 mmol) were added to the solution and stirred at room temperature for 2 h. Then water was added to the solution. The reaction mixture was extracted with CH_2Cl_2, and then washed with a brine solution. The organic layer was separated, dried over anhydrous $MgSO_4$ and concentrated under vacuum to obtain the crude product. The crude product was purified using silica gel column chromatography with hexane/ethyl acetate (75:25), which afforded pure anilido-benzoxazole boron difluoride (ABB) dyes **1**-**6** as yellow-greenish solids in 35-87% yield.

2-(Benzo[*d*]oxazol-2-yl)-*N*-phenylaniline (7): Yield: 214 mg (75%), pale yellow solid. mp 116.0-118.0 °C; ^{1}H NMR (400 MHz, $CDCl_3$, 25 °C): δ = 10.20 (brs, 1H, NH), 8.18 (d, *J* = 7.7 Hz, 1H, Ar-*H*), 7.74-7.72 (m, 1H, Ar-*H*), 7.60-7.58 (m, 1H, Ar-*H*), 7.32-7.25 (m, 8H, Ar-*H*), 7.16-7.13 (m, 1H, Ar-*H*), 6.88 (d, *J* = 7.2 Hz, 1H, Ar-*H*) ppm. ^{13}C NMR (100

MHz, $CDCl_3$, 25 °C): δ = 163.0, 149.4, 145.6, 141.7, 141.3, 132.5, 129.6, 129.3, 125.1, 124.6, 123.8, 122.9, 119.6, 117.8, 114.0, 110.5, 110.1 ppm. IR (KBr film): ν = 3267, 2923, 2840, 2361, 1691, 1531, 1249, 1040, 815, 746 cm^{-1}. HRMS (ESI): *m/z* calcd for $C_{19}H_{14}N_2O$ (M^++H): 287.1179; found 287.1177. The data are in accordance with literature reported values.[24]

2-(Benzo[*d*]oxazol-2-yl)-*N*-(2,6-dimethyl)phenylaniline (8): Yield: 261 mg (83%), white solid. mp 119.0-121.0 °C; ^{1}H NMR (400 MHz, $CDCl_3$, 25 °C): δ = 9.81 (brs, 1H, NH), 8.20 (d, *J* = 7.7 Hz, 1H, Ar-*H*), 7.74-7.71 (m, 1H, Ar-*H*), 7.64-7.61 (m, 1H, Ar-*H*), 7.38-7.35 (m, 2H, Ar-*H*), 7.25-7.20 (m, 4H, Ar-*H*), 6.83-6.79 (m, 1H, Ar-*H*), 6.36 (d, *J* = 8.4 Hz, 1H, Ar-*H*), 2.29 (s, 6H, -CH_3) ppm. ^{13}C NMR (100 MHz, $CDCl_3$, 25 °C): δ = 163.4, 149.3, 147.2, 141.8, 137.7, 137.1, 132.7, 128.9, 128.5, 126.6, 124.8, 124.4, 119.4, 116.1, 112.4, 110.3, 108.2, 18.5 ppm. IR (KBr film): ν = 3268, 3053, 2924, 2361, 1688, 1516, 1255, 1038, 815, 747 cm^{-1}. HRMS (ESI) calcd for $C_{21}H_{19}N_2O$ (M^++H): *m/z* 315.1492; found 315.1494.

2-(Benzo[*d*]oxazol-2-yl)-*N*-(2,6-diethyl)phenylaniline (9): Yield: 277 mg (81%), white solid. mp 115.0-117.0 °C; ^{1}H NMR (400 MHz, $CDCl_3$, 25 °C): δ = 9.81 (brs, 1H, NH), 8.15 (d, *J* = 6.8 Hz, 1H, Ar-*H*), 7.68-7.66 (m, 1H, Ar-*H*), 7.61-7.59 (m, 1H, Ar-*H*), 7.35-7.33 (m, 2H, Ar-*H*), 7.28-7.17 (m, 4H, Ar-*H*), 6.78-6.73 (m, 1H, Ar-*H*), 6.32 (d, *J* = 8.4 Hz, 1H, Ar-*H*), 2.69-2.54 (m, 4H, -CH_2), 1.16 (t, *J* = 7.6 Hz, 6H, -CH_3) ppm. ^{13}C NMR (100 MHz, $CDCl_3$, 25 °C): δ = 163.4, 149.3, 148.0, 143.1, 141.8, 136.4, 132.6, 128.8, 127.1, 126.8, 124.7, 124.3, 119.3, 115.9, 112.5, 110.3, 107.9, 25.0, 14.9 ppm. IR (KBr film): ν = 3267, 2928, 2921, 2361, 1691, 1531, 1253, 1041, 817, 743 cm^{-1}. HRMS (ESI): *m/z* calcd for $C_{23}H_{21}N_2O$ (M^+): 341.1648; found 341.1643.

2-(Benzo[*d*]oxazol-2-yl)-*N*-[2,6-di(propan-2-yl)]phenylaniline (10): Yield: 289 mg (78%), yellow solid. mp 118.0-120.0 °C; ^{1}H NMR (400 MHz, $CDCl_3$, 25 °C): δ = 9.81 (brs, 1H, NH), 8.19 (d, *J* = 6.8 Hz, 1H, Ar-*H*), 7.71-7.69 (m, 1H, Ar-*H*), 7.64-7.61 (m, 1H, Ar-*H*), 7.39-7.30 (m, 5H, Ar-*H*), 7.23-7.20 (m, 1H, Ar-*H*), 6.80-6.76 (m, 1H, Ar-*H*), 6.37 (d, *J* = 8.4 Hz, 1H, Ar-*H*), 3.25-3.18 (m, 2H, -CH), 1.23 (d, *J* = 6.8 Hz, 6H, -CH_3), 1.17 (d, *J* = 6.8 Hz, 6H, -CH_3) ppm. ^{13}C NMR (100 MHz, $CDCl_3$, 25 °C): δ = 163.4, 149.2, 148.6, 147.7, 141.8, 134.9, 132.5, 128.7, 127.6, 124.7, 124.3, 123.9, 119.3, 115.8, 112.7, 110.2, 107.6, 28.5, 24.8, 23.0 ppm. IR (KBr film): ν = 3267, 3049, 2919, 2361, 1679, 1521, 1254, 1041, 815, 745 cm^{-1}. HRMS (ESI) :*m/z* calcd for $C_{25}H_{27}N_2O$ (M^++H): 371.2118; found 371.2118.

2-(Benzo[*d*]oxazol-2-yl)-*N*-(2,6-dichloro)phenylaniline (11): Yield: 283 mg (80%), white solid. mp 161.0-163.0 °C; ^{1}H NMR (400 MHz, $CDCl_3$, 25 °C): δ = 10.20 (brs, 1H, NH), 8.21 (d, *J* = 8.0 Hz, 1H, Ar-*H*), 7.76-7.74 (m, 1H, Ar-*H*), 7.62-7.60 (m, 1H, Ar-*H*), 7.48-7.46 (m, 1H, Ar-*H*), 7.37-7.32 (m, 2H, Ar-*H*), 7.30-7.28 (m, 2H, Ar-*H*), 7.21-7.17 (m, 1H, Ar-*H*), 6.94-6.90 (m, 1H, Ar-*H*), 6.47 (d, *J* = 8.4 Hz, 1H, Ar-*H*) ppm. ^{13}C NMR (100 MHz, $CDCl_3$, 25 °C): δ = 162.8, 149.3, 144.9, 141.6, 135.9, 134.6, 132.2, 128.9, 128.8, 127.2, 125.0, 124.4, 119.6, 118.0, 113.5, 110.3, 109.7 ppm. IR (KBr film): ν = 3429, 3254, 2920, 2361, 1652, 1516, 1251, 1042, 812, 778, 745 cm^{-1}. HRMS (ESI): *m/z* calcd for $C_{19}H_{12}Cl_2N_2O$ (M^++Na): 354.0219; found 377.0218.

2-(Benzo[*d*]oxazol-2-yl)-*N*-(2,6-dibromo)phenylaniline (12): Yield: 376 mg (85%), white solid. mp 148.0-150.0 °C; ^{1}H NMR (400 MHz, $CDCl_3$, 25 °C): δ = 10.21 (brs, 1H, NH), 8.23 (d, *J* = 7.6 Hz, 1H, Ar-*H*), 7.78-7.76 (m, 1H, Ar-*H*), 7.70-7.68 (m, 2H, Ar-*H*), 7.63-7.60 (m, 1H, Ar-*H*), 7.39-7.29 (m, 3H, Ar-*H*), 7.08-7.04 (m, 1H, Ar-*H*), 6.96-6.92 (m, 1H, Ar-*H*), 6.45 (d, *J* = 8.4 Hz, 1H, Ar-*H*) ppm. ^{13}C NMR (100 MHz, $CDCl_3$, 25 °C): δ = 162.8, 149.3, 144.9, 141.6, 138.5, 132.8, 132.3, 128.9, 128.5, 125.4, 124.9, 124.4, 119.6, 117.9, 113.4, 110.4, 109.5 ppm. IR (KBr film): ν = 3438, 3254, 2923, 2361, 1657, 1531, 1261, 1055, 821, 668, 745 cm^{-1}. HRMS (ESI): *m/z* calcd for $C_{19}H_{12}Br_2N_2O$ (M^++Na+2): 464.9209; found 466.9191.

Synthesis of 1: Yield: 117 mg (35%), yellow-green solid. mp 231.0-233.0 °C; ^{1}H NMR (400 MHz, $CDCl_3$, 25 °C): δ = 8.18 (dd, ^3J = 8.0 Hz, ^1J = 1.4 Hz, 1H, Ar-*H*), 7.74-7.71 (m, 1H, Ar-*H*), 7.60-7.58 (m, 1H, Ar-*H*), 7.40-7.31 (m, 8H, Ar-*H*), 7.14-7.11 (m, 1H, Ar-*H*), 6.90-6.86 (m, 1H, Ar-*H*) ppm. ^{13}C NMR (100 MHz, $CDCl_3$, 25 °C): δ = 162.8, 149.2, 141.5, 141.1, 132.3, 129.4, 129.1, 124.9, 124.4, 123.6, 122.8, 119.4, 117.6, 113.9, 110.3, 109.9 ppm. IR (KBr film): ν = 2923, 2840, 2361, 1692, 1534, 1261, 1073, 821, 670 cm^{-1}. ^{11}B NMR (160 MHz, $CDCl_3$, 25 °C): δ = 2.35 (t, $^1J_{B\text{-}F}$ = 25.6 Hz, 1B) ppm. ^{19}F NMR (375 MHz, $CDCl_3$, 25 °C): δ = -131.7 (dd, $^1J_{F\text{-}B}$ = 15.0 Hz, $^1J_{F\text{-}F}$ = 33.8 Hz, 2F) ppm. HRMS (ESI): *m/z* calcd for $C_{19}H_{13}BF_2N_2O$ (M^++Na): 357.0985; found 357.0997.

Synthesis of 2: Yield: 319 mg (88%), yellow-green solid. mp 245.0-247.0 °C; ^{1}H NMR (400 MHz, $CDCl_3$, 25 °C): δ = 7.99 (d, *J* = 1.2 Hz, 1H, Ar-*H*), 7.97-7.93 (m, 1H, Ar-*H*), 7.72-7.70 (m, 1H, Ar-*H*), 7.53-7.51 (m, 2H, Ar-*H*), 7.34-7.30 (m, 1H, Ar-*H*), 7.19 (s, 3H, Ar-*H*), 6.79-6.75 (m, 1H, Ar-*H*), 6.26 (d, *J* = 8.8 Hz, 1H, Ar-*H*), 2.19 (s, 6H, -CH_3) ppm. ^{13}C NMR (100 MHz, $CDCl_3$, 25 °C): δ = 161.3, 150.7, 148.6, 138.2, 138.1, 137.0, 131.5, 128.8, 127.1, 126.8, 126.7, 126.4, 116.9, 116.1, 114.8, 111.3, 100.9, 18.2 ppm. IR (KBr film): ν = 2923, 2840, 2361, 1691, 1534, 1291, 1066, 819, 666 cm^{-1}. ^{11}B NMR (160 MHz, $CDCl_3$, 25 °C): δ = 2.04 (t, $^1J_{B\text{-}F}$ = 25.6 Hz, 1B) ppm. ^{19}F NMR (375 MHz, $CDCl_3$, 25 °C): δ = -132.8 (dd, $^1J_{F\text{-}B}$ = 15.0 Hz, $^1J_{F\text{-}F}$ = 48.8 Hz, 2F) ppm. HRMS (ESI): *m/z* calcd for $C_{21}H_{17}BF_2N_2O$ (M^++K): 401.1037; found 401.1034.

Synthesis of 3: Yield: 332 mg (85%), yellow-green solid. mp 238.0-240.0 °C; ^{1}H NMR (400 MHz, $CDCl_3$, 25 °C): δ = 7.98 (d, *J* = 1.2 Hz, 1H, Ar-*H*), 7.97-7.93 (m, 1H, Ar-*H*), 7.71-7.69 (m, 1H, Ar-*H*), 7.52-7.50 (m, 2H, Ar-*H*), 7.34-7.27 (m, 4H, Ar-*H*), 6.78-6.76 (m, 1H, Ar-*H*), 6.28 (d, *J* = 8.8 Hz, 1H, Ar-*H*), 2.73-2.67 (m, 2H, -CH_2), 2.52-2.47 (m, 2H, -CH_2), 1.11 (t, *J* = 6.8 Hz, 6H, -CH_3) ppm. ^{13}C NMR (100 MHz, $CDCl_3$, 25 °C): δ = 161.5, 151.6, 148.7, 143.4, 136.9, 136.6, 131.5, 127.4, 126.8, 126.6, 126.4, 126.3, 116.9, 116.1, 115.7, 111.2, 100.8, 23.5, 14.4 ppm. IR (KBr film): ν = 2923, 2840, 2361, 1643, 1533, 1296, 1071, 820, 670 cm^{-1}. ^{11}B NMR (160 MHz, $CDCl_3$, 25 °C): δ = 1.94 (t, $^1J_{B\text{-}F}$ = 25.6 Hz, 1B) ppm. ^{19}F NMR (375 MHz, $CDCl_3$, 25 °C): δ = -132.3 (br, m, 2F) ppm. HRMS (ESI): *m/z* calcd for $C_{23}H_{21}BF_2N_2O$ (M^++K): 429.1351; found 429.1349.

Synthesis of 4: Yield: 293 mg (70%), yellow-green solid. mp 248.0-250.0 °C; ^{1}H NMR (400 MHz, $CDCl_3$, 25 °C): δ = 7.99-7.94 (m, 2H, Ar-*H*), 7.71-7.69 (m, 1H, Ar-*H*), 7.52-7.50 (m, 2H, Ar-*H*), 7.39-7.37 (m, 1H, Ar-*H*), 7.31-7.27 (m, 3H, Ar-*H*), 6.77-6.74 (m, 1H, Ar-*H*), 6.32 (d, *J* = 8.8 Hz, 1H, Ar-*H*), 3.13-3.09 (m, 2H, -CH), 1.26-1.24 (m, 6H, -CH_3), 0.98 (d, *J* = 7.56 Hz, 6H, -CH_3) ppm. ^{13}C NMR (100 MHz, $CDCl_3$, 25 °C): δ = 161.3, 152.0, 148.7, 148.3, 136.2, 135.0, 131.6, 127.9, 126.7, 126.6, 126.2, 124.5, 117.0, 116.5, 116.1, 111.2, 100.7, 28.2, 25.1, 24.0 ppm. IR (KBr

film): ν = 2924, 2840, 2361, 1693, 1532, 1291, 1072, 819, 746, 674 cm^{-1}. ^{11}B NMR (160 MHz, $CDCl_3$, 25 °C): δ = 2.33 (t, $^1J_{B\text{-}F}$ = 22.4 Hz, 1B) ppm. ^{19}F NMR (375 MHz, $CDCl_3$, 25 °C): δ = -131.3 (br, m, 2F) ppm. HRMS (ESI): *m/z* calcd for $C_{25}H_{25}BF_2N_2O$ (M^++K): 457.1664; found 457.1659.

Synthesis of 5: Yield: 342 mg (85%), green-yellow solid. mp 294.0-296.0 °C; ^1H NMR (400 MHz, $CDCl_3$, 25 °C): δ = 8.04 (d, *J* = 1.2 Hz, 1H, Ar-*H*), 8.03-7.94 (m, 1H, Ar-*H*), 7.73-7.70 (m, 1H, Ar-*H*), 7.54-7.50 (m, 4H, Ar-*H*), 7.30-7.27 (m, 1H, Ar-*H*), 7.25-7.24 (m, 1H, Ar-*H*), 6.90-6.86 (m, 1H, Ar-*H*), 6.31 (d, *J* = 8.8 Hz, 1H, Ar-*H*) ppm. ^{13}C NMR (100 MHz, $CDCl_3$, 25 °C): δ = 161.3, 149.8, 148.7, 137.1, 137.0, 136.5, 131.4, 129.1, 128.7, 126.9, 126.6, 117.4, 117.0, 114.9, 111.3, 102.1 ppm. IR (KBr film): ν = 2923, 2840, 2361, 1693, 1531, 1261, 1073, 821, 666 cm^{-1}. ^{11}B NMR (160 MHz, $CDCl_3$, 25 °C): δ = 1.77 (t, $^1J_{B\text{-}F}$ = 27.2 Hz, 1B) ppm. ^{19}F NMR (375 MHz, $CDCl_3$, 25 °C): δ = -133.1 (dd, $^1J_{F\text{-}B}$ = 20.0 Hz, $^1J_{F\text{-}F}$ = 52.0 Hz, 2F) ppm. HRMS (ESI): *m/z* calcd for $C_{19}H_{11}BCl_2F_2N_2O$ (M^++Na): 425.0205; found 425.0221.

Synthesis of 6: Yield: 426 mg (87%), yellow solid. mp 283.0-285.0 °C; ^1H NMR (400 MHz, $CDCl_3$, 25 °C): δ = 8.03 (d, *J* = 1.2 Hz, 1H, Ar-*H*), 7.97-7.95 (m, 1H, Ar-*H*), 7.73-7.71 (m, 3H, Ar-*H*), 7.54-7.52 (m, 2H, Ar-*H*), 7.44-7.40 (m, 1H, Ar-*H*), 7.13-7.10 (m, 1H, Ar-*H*), 6.92-6.87 (m, 1H, Ar-*H*), 6.32 (d, *J* = 8.8 Hz, 1H, Ar-*H*) ppm. ^{13}C NMR (100 MHz, $CDCl_3$, 25 °C): δ = 161.3, 149.6, 148.7, 139.3, 137.0, 133.1, 131.4, 129.5, 127.1, 126.9, 126.6, 117.5, 117.1, 115.2, 111.3, 102.2 ppm. IR (KBr film): ν = 2923, 2840, 2361, 1646, 1532, 1261, 1062, 819, 666 cm^{-1}. ^{11}B NMR (160 MHz, $CDCl_3$, 25 °C): δ = 1.74 (t, $^1J_{B\text{-}F}$ = 25.6 Hz, 1B) ppm. ^{19}F NMR (375 MHz, $CDCl_3$, 25 °C): δ = -132.7 (dd, $^1J_{F\text{-}B}$ = 15.0 Hz, $^1J_{F\text{-}F}$ = 33.8 Hz, 2F) ppm. HRMS (ESI): *m/z* calcd for $C_{19}H_{11}BBr_2F_2N_2O$ (M^++K): *m/z* 528.8934; found 532.8909.

Acknowledgements

We are grateful to the National Science Council of Taiwan (Grant No. 98-2119-M-003-002-MY3). We also acknowledge Prof. Yang, J.-S. at National Taiwan University and Prof. Sun, S.-S. at Academia Sinica for the facility for solid-state and life time fluorescence measurements, respectively.

†Electronic Supplementary Information (ESI) available: ^1H, ^{13}C, ^{19}F and ^{11}B NMR spectra, DFT calculation data, X-ray crystal structures, UV-vis absorption and fluorescence spectra and tables of properties. See DOI: 10.1039/b000000x/

Notes and references

[a]*Department of Chemistry, National Taiwan Normal University, Taipei, 11677, Taiwan (R.O.C.). Fax: (+886) 2-29324249; Tel: (+886) 2-77346133; E-mail: wzlee@ntnu.edu.tw.*

[b] *Instrumentation Center, Department of Chemistry, National Taiwan Normal University, Taipei 11677, Taiwan.*

1 (a) A. Mishra and P. Bäuerle, *Angew. Chem., Int. Ed.,* 2012, **51**, 2020; (b) L. Xiao, Z. Chen, B. Qu, J. Luo, S. Kong, Q. Gong and J. Kido, *Adv. Mater.,* 2011, **23**, 926; (c) C. Chen, *Chem. Mater.,* 2004, **16**, 4389.

2 (a) Y. Zhou, Z. Xu and J. Yoon, *Chem. Soc. Rev.,* 2011, **40**, 2222; (b) M. E. Moragues, R. Martinez-manez and F. Sancenon, *Chem. Soc. Rev.,* 2011, **40**, 2593; (c) Q. Zhao, C. Huang and F. Li, *Chem. Soc. Rev.,* 2011, **40**, 2508.

3 (a) X. Y. Liu, D. R. Bai and S. N. Wang, *Angew. Chem., Int. Ed.,* 2006, **45**, 5475; (b) S Yamaguchi, S. Akiyama and K. Tamao, *J. Am. Chem. Soc.,* 2001, **123**, 11372; (c) Y. Kubo, M. Yamamoto, M. Ikeda, M. Takeuchi, S. Shinkai, S. Yamaguchi and K. Tamao, *Angew. Chem., Int. Ed.,* 2003, **42**, 2036.

4 (a) J. Killoran, L. Allen, J. F. Gallagher, W. M. Gallagher and D. F. O'Shea, *Chem. Commun.,* 2002, 1862; (b) W. Yang, H. He and D. G. Drueckhammer, *Angew. Chem., Int. Ed.,* 2001, **40**, 1714; (c) N. DiCesare and J. R. Lakowicz, *J. Phys. Chem.,* 2001, **105**, 6834.

5 (a) M. S. T. Gonçalves, *Chem. Rev.,* 2009**, 109**, 190; (b) S. R. Trenor, A. R. Shultz, B. L. Love and T. E. Long, *Chem. Rev.,* 2004, **104**, 3059.

6 (a) H. Zheng, X.-Q. Zhan, Q.-N. Biana and X.-J. Zhanga, *Chem. Commun.,* 2013, **49**, 429; (b) W. Shi and H. Ma, *Chem. Commun.,* 2012, **48**, 8732.

7 A. Mishra, R. K. Behera, P. K. Behera, B. K. Mishra and G. E. Behera, *Chem. Rev.,* 2000, **100,** 1973.

8 M. Beija, C. A. M. Afonso and J. M. G. Martinho, *Chem. Soc. Rev.,* 2009, **38**, 2410.

9 D. T. Quang and J. S. Kim, *Chem. Rev.,* 2010, **110**, 6280.

10 (a) A. Loudet and K. Burgess, *Chem. Rev.,* 2007, **107**, 4891; (b) G. Ulrich, R. Ziessel and A. Harriman, *Angew. Chem., Int. Ed.*, 2008, **47**, 1184; (c) N. Boens, V. Leen and W. Dehaen, *Chem. Soc. Rev.,* 2012, **41**, 1130.

11 (a) D. P. Murale, K. M. Lee, K. Kima and D. G. Churchill, *Chem. Commun.,* 2011, **47**, 12512; (b) F. Camerel, L. Bonardi, M. Schmutz and R. Ziessel, *J. Am. Chem. Soc.,* 2006, **128**, 4548; (c) G.-L. Fu, H. Pan, Y.-H. Zhao and C.-H. Zhao, *Org. Biomol. Chem.,* 2011, **9**, 8141; (d) R. Guliyev, A. Coskun and E. U. Akkaya, *J. Am. Chem. Soc.,* 2009, **131**, 9007.

12 (a) J. F. Lovell, T. W. B. Liu, J. Chen and G. Zheng, *Chem. Rev.,* 2010, **110**, 2839; (b) A. Kamkaew, S. H. Lim, H. B. Lee, L. V. Kiew, L. Y. Chung and K. Burgess, *Chem. Soc. Rev.,* 2013, **42**, 77.

13 (a) J. Bañuelos, V. Martín, C. F. A. Gómez-Durán, I. J. A. Córdoba, E. Peña-Cabrera, I. García-Moreno, Á. Costela, M. E. Pérez-Ojeda, T. Arbeloa and I. López Arbeloa, *Chem. Eur. J.,* 2011, **17**, 7261; (b) Y. Xiao, D. Zhang, X. Qian, A. Costela, I. García-Moreno, V. Martin, M. E. Perez-Ojeda, J. Banuelos, L. Gartzia and I. LópezArbeloa, *Chem. Commun.,* 2011, **47**, 11513.

14 (a) S. Ertan-Ela, M. D. Yilmaz, B. Icli, Y. Dede, S. Icli and E. U. Akkaya, *Org. Lett.,* 2008, **10**, 3299; (b) T. Rousseau, A. Cravino, T. Bura, G. Ulrich, R. Ziessel and J. Roncali, *Chem. Commun.,* 2009, 1673; (c) M. Mao, J.-B. Wang, Z.-F. Xiao, S.-Y. Dai and Q.-H. Song, *Dyes Pigm.,* 2012, **94**, 224.

15 (a) F. Ito, T. Nagai, Y. Ono, K. Yamaguchi, H. Furuta and T. Nagamura, *Chem. Phys. Lett.,* 2007, **435**, 283; (b) W. Qin, T. Rohand, M. Baruah, A. Stefan, M. Van der Auweraer, W. Dehaen and N. Boens, *Chem. Phys. Lett.,* 2006, **420**, 562.

16 (a) T. Ozdemir, S. Atilgan, I. Kutuk, L. T. Yildirim, A. Tulek, M. Bayindir and E. U. Akkaya, *Org. Lett.,* 2009, **11**, 2105; (b) D. Zhang, Y. Wen, Y. Xiao, G. Yu, Y. Liu and X. Qian, *Chem.*

Commun., 2008, 4777; (c) A. Hepp, G. Ulrich, R. Schmechel, H. Seggern and R. Ziessel, *Synth. Met.,* 2004, **146**, 11.

17 (a) G. Fu, H. Pan, Y. Zhao and C. Zhao, *Org. Biomol. Chem.,* 2011, **9**, 8141; (b) H. Xi, C. Yuan, Y. Li, Y. Liu and X. Tao, *J. Phys. Chem. C,* 2011, **115**, 19947; (c) H. Lu, Q. Wang, L. Gai, Z. Li, Y. Deng, X. Xiao, G. Lai and Z. Shen, *Chem. Eur. J.,* 2012, **18**, 7852; (d) L. Gai, H. Lu, B. Zou, G. Lai, Z. Shen and Z. Li, *RSC Adv.,* 2012, **2**, 8840; (e) H. Xi, C.-X. Yuan, Y.-X. Li, Y. Liu and X.-T. Tao, *CrystEngComm*, 2012, **14**, 2087.

18 (a) A. Martin, C. Long, R. J. Forster and T. E. Keyes, *Chem. Commun.,* 2012, **48**, 5617; (b) J. C. Er, M. K. Tang, C. G. Chia, H. Liew, M. Vendrell and Y.-T. Chang, *Chem. Sci.,* 2013, **4,** 2168.

19 J. F. Araneda, W. E. Piers, B. Heyne, M. Parvez and R. McDonald, *Angew. Chem.,* 2011, **123**, 12422; *Angew. Chem. Int. Ed.,* 2011, **50**, 12214.

20 For some examples, see: (a) Y. Kubota, S. Tanaka, K. Funabiki and M. Matsui, *Org. Lett.,* 2012, **14**, 4682; (b) Y. Kubota, Y. Ozaki, K. Funabiki and M. Matsui, *J. Org. Chem.,* 2013, **78**, 7058; (c) Kubota, Y.; Sakuma, Y.; Funabiki, K.; Matsui, M. *J. Phys. Chem. A,* 2014, **118** 8717; (d) D. Frath, J. Massue, G. Ulrich and R. Ziessel, *Angew. Chem. Int. Ed.,* 2014, **53**, 2290; (e) J. Massue, D. Frath, P. Retailleau, G. Ulrich and R. Ziessel, *Chem. Eur. J.,* 2013, **19**, 5375; (f) M. Santra, H. Moon, M.-H. Park, T.-W. Lee, Y. K. Kim and K. H. Ahn, *Chem. Eur. J.,* 2012, **18**, 9886; (g) Y. Zhou, Y. Xiao, D. Li, M. Fu and X. Qian, *J. Org. Chem.,* 2008, **73**, 1571; (h) Y. Zhou, Y. Xiao, S. Chi, X. Qian, *Org. Lett*., 2008, **10**, 633; (i) K. Perumal, J. A. Garg, O. Blacque, R. Saiganesh, S. Kabilan, K. K. Balasubramanian and K. Venkatesan, *Chem. Asian J.,* 2012, **7**, 2670; (j) Y. Rao, H. Amarne and S. Wang, *Coord. Chem. Rev.,* 2012, **256**, 759; (k) Y. Yang, X. Su, C. N. Carroll and I. Aprahamian, *Chem. Sci.,* 2012, **3**, 610; (l) Z. Zhang, B. Xu, J. Su, L. Shen, Y. Xie and H. Tian, *Angew. Chem.,* 2011, **123**, 11858; (m) D. Li, Y. Yuan, H. Bi, D. D. Yao, X. J. Zhao, W. J. Tian, Y. Wang and H. Y. Zhang, *Inorg. Chem.,* 2011, **50**, 4825; (n) A. Wakamiya, K. Mori and S. Yamaguchi, *Angew. Chem., Int. Ed.,* 2007, **46**, 4273; (o) J. Wang, Y. Zhao, C. Dou, H. Sun, P. Xu, K. Ye, J. Zhang, S. Jiang, F. Li and Y. Wang, *J. Phys. Chem. B,* 2007, **111**, 5082; (p) A. Job, A. Wakamiya, G. Kehr, G. Erker and S. Yamaguchi, *Org. Lett.,* 2010, **12**, 5470;

21 (a) M. J. Kwak and Y. Kim, *Bull. Korean Chem. Soc.,* 2009, **30**, 2865; (b) J. Massue, P. Retailleau, G. Ulrich and R. Ziessel, *New J. Chem.,* 2013, **37**, 1224; (c) B. L. Guennic, S. Chibani, A. Charaf-Eddin, J. Massue, R. Ziessel, G. Ulrich and D. Jacquemin, *Phys. Chem. Chem. Phys.,* 2013, **15**, 7534; (d) J. Massue, D. Frath, P. Retailleau, G. Ulrich and R. Ziessel, *Org. Lett.,* 2012, **14**, 230.

22 (a) N. Gao, C. Cheng, C. Yu, E. Hao, S. Wang, J. Wang, Y. Wei, X. Mu and L. Jiao, *Dalton Trans.,* 2014, **43**, 7121; (b) C. Yu, L. Jiao, P. Zhang, Z. Feng, C. Cheng, Y. Wei, X. Mu, and E. Hao, *Org. Lett.*, 2014, **16**, 3048.

23 (a) D. Li, K. Wang, S. Huang, S. Qu, X. Liu, Q. Zhu, H. Zhang and Y. Wang, *J. Mater. Chem.,* 2011, **21**, 15298; (b) Z. L. Zhang, H. Bi, Y. Zhang, D. D. Yao, H. Z. Gao, Y. Fan, H. Y. Zhang, Y. Wang, Y. P. Wang, Z. Y. Chen and D. G. Ma, *Inorg. Chem.,* 2009, **48**, 7230; (c) D. Li, Z. Zhang, S. Zhao, Y. Wang and H. Zhang, *Dalton Trans.,* 2011, **40**, 1279; (d) D. Li, H. Zhang, C. Wang, S. Huang, J. Guo and Y. Wang, *J. Mater. Chem.*, 2012, **22**, 4319.

24 (a) S.-F. Liu, Q. Wu, H. L. Schmider, H. Aziz, N.-X. Hu, Z. Popović and S. Wang, *J. Am. Chem. Soc.,* 2000, **122**, 3671; (b) Q. Wu, M. Esteghamatian, N.-X. Hu, Z. Popovic, G. Enright, Y. Tao, M. Diorio and S. Wang, *Chem. Mater.,* 2000, **12**, 79; (c) Q. Liu, M. S. Mudadu, H. Schmider, R. Thummel, Y. Tao and S. Wang, *Organometallics*, 2002, **21**, 4743; (d) Q. D. Liu, M. S. Mudadu, R. Thummel, Y, Tao and S. Wang, *Adv. Funct. Mater.,* 2005, **15**, 143; (e) Y. Cui, Q. D. Liu, D. R. Bai, W. L. Jia, Y. Tao and S. Wang, *Inorg. Chem.,* 2005, **44**, 601. (f) Y.-L. Rao and S. Wang, *Inorg. Chem.,* 2011, **50**, 12263; (g) H.-Y. Chen, Y. Chi, C.-S. Liu, J.-K. Yu, Y.-M. Cheng, K.-S. Chen, P.-T. Chou, S.-M. Peng, G.-H. Lee, A. J. Carty, S.-J. Yeh and C.-T. Chen, *Adv. Funct. Mater.,* 2005, **15**, 567.

25 V. Kavala, D. Janreddy, M. J. Raihan, C.-W. Kuo, C. Ramesh and C.-F. Yao, *Adv. Synth. Catal.,* 2012, **354**, 2229.

26 (a) S. Hamai and F. Hirayama, *J. Phys. Chem.,* 1983, **87**, 83; (b) A. M. Brouwer, *Pure Appl. Chem.,* 2011, **83**, 2213.

27 T. L. Stottand and M. O. Wolf, *J. Phys. Chem. B,* 2004, **108**, 18815.

28 (a) X. M. Liu, W. Gao, Y. Mu, G. H. Li, L. Ye, H. Xia, Y. Ren and S. H. Feng, *Organometallics,* 2005, **24**, 1614; (b) X. M. Liu, H. Xia, W. Gao, L. Ye, Y. Mu, Q. Su and Y. Ren, *Eur. J. Inorg. Chem.,* 2006, 1216; (c) Y. Ren, X. M. Liu, H. Xia, L. Ye and Y. Mu, *Eur. J. Inorg. Chem.,* 2007, 1808; (d) Z. Li, Y. Dong, B. X. Mi, Y. H. Tang, M. Haussler, H. Tong, Y. P. Dong, J. W. Y. Lam, Y. Ren, H. H. Y. Sung, K. S. Wong, P. Gao, I. D. Williams, H. S. Kwok and B. Z. Tang, *J. Phys. Chem. B,* 2005, **109**, 10061.

29 K. Kudo, A. Momotake, Y. Kanna, Y. Nishimura and T. Arai, *Chem. Commun.* 2011, **47**, 3867.

30 A. Gorman, J. Killoran, C. O'Shea, T. Kenna, W. M. Gallagher and D. F. O'Shea, *J. Am. Chem. Soc.,* **2004**, **126**, 10619.

31 H. Li, Z. Chi, X. Zhang, B. Xu, S. Liu, Y. Zhang and J. Xu, *Chem. Commun.,* 2011, 11273.

Table of contents

Synthesis, Crystal Structures, Electrochemical and Photophysical Properties of Anilido-Benzoxazole Boron Difluoride (ABB) Complexes

Yedukondalu Meesala, Veerababurao Kavala, Hao-Ching Chang, Ting-Shen Kuo, Ching-Fa Yao, Way-Zen Lee**

A new series of four-ring-fused π-conjugated anilido-benzoxazole boron difluoride (ABB) dyes have been synthesized by employing unsymmetrical bidentate ligand in a mild reaction condition. The dyads exhibited very bright luminescence in solution (Φ_f = 0.45-0.96 in CH_2Cl_2) and in the solid-state (Φ_f = 0.07-0.37). These dyads showed a larger Stokes shift (58-101 nm) than well-known boron dipyrromethene dyes (8-12 nm, in most cases).